Reshaping of femtosecond pulses by the Gouy phase shift

Z. L. Horváth and Zs. Bor
Department of Optics and Quantum Electronics, JATE University, P.O. Box 406, H-6701 Szeged, Hungary
(Received 10 November 1998)

It is shown that because of the phase anomaly a femtosecond pulse propagates on the optical axis with a velocity greater than c in the vicinity of the focus not only for large but also small values of the Fresnel number. The group velocity is calculated and its physical meaning discussed. Analytical expressions are derived for the electric field. The causality of the system is proved. The mechanism of the superluminality is a reshaping process caused by the interference. Contrary to other superluminal phenomena, the superluminal propagation occurs in a classically *not* forbidden region. [S1063-651X(99)11108-5]

PACS number(s): 42.25.Bs, 03.65.Bz, 42.25.Fx

I. INTRODUCTION

It is well known that the phase fronts of a converging spherical wave diffracted at a circular aperture differs from the spherical wave fronts of geometrical optics. The phase difference discovered by Gouy is called phase anomaly (or Gouy shift) [1,2]. The phase anomaly occurs for both uniform converging wave and Gaussian beam, but in the case of weak truncation of the incident Gaussian beam the phase anomaly is much more well behaved than the one for a uniform converging spherical wave. Pulse propagation in dispersive medium and diffraction of pulses at a hole in an opaque screen are analogous phenomenon [3]. It is well-known that the group velocity in dispersive medium can exceed c [5–9]. The diffraction induces a frequency dependent phase distribution in a dispersionless media, even in vacuum. Because of the presence of the frequency dependent phase anomaly and since the geometrical phase fronts move with speed of c, it is a quite obvious assumption that the phase and the group velocity differs from c.

In Ref. [4] the group velocity was calculated in the neighborhood of the focal point of an aberration-free lens illuminated by a Gaussian beam with beam waist w carrying a femtosecond pulse with central wavelength λ_0. The analysis was confined to weak truncation of the incident beam and the Fresnel number associated with the waist of the incident beam was assumed to be large compared to unity (then the focal shift is negligible [26,27]). The group velocity on the optical axis is given by [4]

$$v_g(z)=\frac{[1+[\pi N_w z/f]^2]^2 c}{[1+[\pi N_w z/f]^2]^2-[1-[\pi N_w z/f]^2]\frac{\vartheta^2}{2}}$$

$$=\frac{[1+[\vartheta^2\zeta_0]^2]^2 c}{[1+[\vartheta^2\zeta_0]^2]^2-[1-[\vartheta^2\zeta_0]^2]\frac{\vartheta^2}{2}}, \qquad (1)$$

where z is the coordinate of point P measured from the focus (Fig. 1), f is the focal length, N_w is the Fresnel number associated with the waist at λ_0 given by $N_w=w^2/(\lambda_0 f)$, $\vartheta=w/f$ is the divergence of the focused beam and $\zeta_0=\pi z/\lambda_0$ is a dimensionless variable. The most exciting consequence of Eq. (1) is that the propagation is superluminal [4] within the Rayleigh range defined by $(-z_{f0},z_{f0})$, where $z_{f0}=\lambda_0/(\pi\vartheta^2)$ is the Rayleigh length of the focused beam at λ_0. We use the word *superluminal* in this paper in the sense that $v_g>c$.

There are several mechanisms that leads to superluminal propagation. Surveys of the topic can be found in Refs. [7,8]. The group velocity can behave abnormal in dispersive media in regions of anomalous dispersion [5–9]. Superluminal group velocity can also occur in media with population inversion [7]. In this case two types of inversion have been investigated: the steady-state inversion and the sudden inversion. In case of steady-state inversion the superluminality is caused by the sign change of the real part of the linear susceptibility [7,10–14]. In case of sudden inversion the coupling between the electromagnetic field and atomic polarization waves leads to tachyonlike excitations with superluminal group velocities [7,15]. Superluminal propagation has been associated with quantum tunneling and its electromagnetic analogues [7,8]. Superluminal group velocities have been observed using microwaves [7,8,16–19] and light pulses passing through a dielectric mirror [7,8,20,21]. Superluminal propagation has also been reported in periodic or quasiperiodic multilayer systems [7,22–24] and optical phase conjugators [25].

The superluminality occurred in the tunneling and the microwave experiments is often attributed to evanescent waves. Other types of tunnelinglike phenomena occur in optics, for

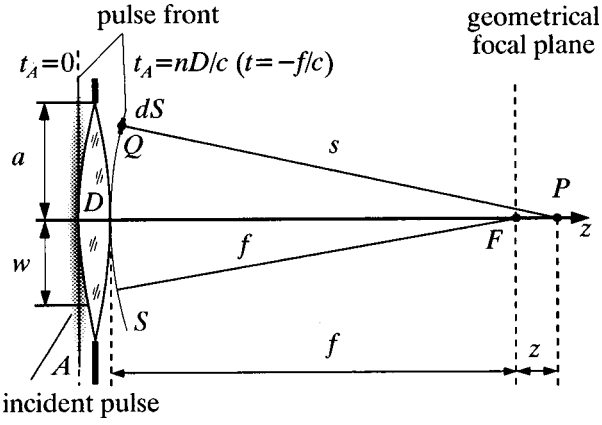

FIG. 1. Notations relating to the calculations.

example, propagation of light diffracted at a straight edge into the shadow region, or propagation of light outside of the allowed orders of a grating or a Fabry-Perot interferometer [7]. These phenomena are all classically forbidden (forbidden in the sense of the classical mechanics and the geometrical optics). One of the interest of our article is that it describes a phenomenon in which the superluminal propagation occurs in a region allowed by the geometrical optics and the light propagates in a dispersionless medium (vacuum).

In Ref. [4] little attention has been paid to the causality and the pulse shape. It is an interesting question whether the pulse propagates indeed with the group velocity and, meanwhile, pulse distortions occur. In the rest of this paper the electric field of the pulse is calculated on the optical axis and a generalization of Eq. (1) is derived for arbitrary N_w (i.e., the focal shift is taken into account). We will consider the problem of causality and examine the velocity and the distortion of the pulse.

II. ELECTRIC FIELD ON THE OPTICAL AXIS

Consider a thin lens illuminated by a (spatially) Gaussian beam carrying a femtosecond pulse having temporal duration of τ (full width at half-maximum in intensity) and central wavelength λ_0. We assume that the waist of the beam is located in the input plane of the lens (plane A in Fig. 1.) and the lens fills a circular aperture of radius a in an opaque screen. We suppose that the electric field in plane A is given by

$$E_i(\rho,t_A)=E_0e^{-(\rho/w)^2}h(t_A)=E_0e^{-(\rho/w)^2}s(t_A)e^{i\omega_0 t_A}, \quad (2)$$

where E_0 is a constant, w is the beam waist, $s(t)$ is the envelope and $\omega_0=2\pi c/\lambda_0$ is the central frequency of the pulse, $h(t)=s(t)e^{i\omega_0 t}$ describes the temporal dependence of the electric field. Here ρ is the distance measured from the optical axis and t_A is the local time in plane A. We assume that the pulse front reaches plane A at the moment of $t_A=0$. In order to study the pure effect caused by the phase anomaly, we suppose that the lens is free of aberrations of any type.

We construct the focused field as the superposition monochromatic Fourier components $U(P,\omega)$:

$$E(P,t_A)=\mathcal{F}^{-1}_{t_A\omega}\{U(P,\omega)\}=\frac{1}{2\pi}\int_{-\infty}^{\infty}U(P,\omega)e^{i\omega t_A}d\omega, \quad (3)$$

where the symbol $\mathcal{F}^{-1}$ denotes the inverse Fourier transform, the subscripts of $\mathcal{F}$ indicates the conjugate variables of the transformation. The lens converts the plane phase fronts into spherical phase fronts of radius f centered at the geometrical focal point F, so the monochromatic components at a typical point Q of spherical surface S (Fig. 1) may be expressed as

$$U_S(Q)=E_0e^{-(\rho/w)^2}H(\omega)e^{-ik\Delta}=fH(\omega)e^{-ik(\Delta+f)}E_0e^{-(\rho/w)^2}\frac{e^{ikf}}{f}, \quad (4)$$

where $H(\omega)=\mathcal{F}_{t\omega}\{h(t)\}$ [i.e., the Fourier transform of $h(t)$], $k=2\pi/\lambda=\omega/c$ is the wave number. Here $k\Delta=knD$ is the phase shift introduced by the lens, where n is the refractive index and D is the axial thickness of the lens. The spectral components behind the lens at a point P not too close to the plane of the aperture can be calculated from the diffraction integral [1]. If $\lambda\ll a$ and $(a/f)^2\ll 1$ the spectral components are given by [27]

$$U(P,\omega)=fH(\omega)e^{-ik(\Delta+f)}\left[\frac{ikE_0}{2\pi}\frac{e^{ikf}}{f}\int\int_S e^{-(\rho/w)^2}\frac{e^{iks}}{s}dS\right], \quad (5)$$

where s is the distance QP and the integration extends over the spherical calotte generated by the aperture and the focal point F, having radius f. The expression between the brackets in Eq. (5) has already been calculated in Ref. [27]. If $-f/2\leqslant z$ and $f\cdot K(N_a)\leqslant z$ the monochromatic field at a point P on the optical axis is given by

$$U(z,\omega)=fH(\omega)e^{-ik(\Delta+f)}\left[-iE_0\left(\frac{\pi N_a-u}{f}\right)\times\frac{e^{-\kappa+iu}-1}{\kappa-iu}e^{-ikf[u/(\pi N_a-u)]}\right] \quad (6a)$$

$$=fH(\omega)e^{-ik(\Delta+f)}\left[-iE_0\frac{\omega}{c}\frac{a^2}{2f(f+z)}\times\frac{e^{-\kappa+iu}-1}{\kappa-iu}e^{-ikz}\right], \quad (6b)$$

where $K(N_a)$ is the root of the equation of $8(1+x)^3=x^2N_a$ (see Fig. 2 in Ref. [27]), $N_a=a^2/(\lambda f)$ is the Fresnel number associated with the radius of the aperture, $\kappa=(a/w)^2$ is the coefficient of truncation of the incident beam and $u=u(z,\omega)$ is a dimensionless variable defined by

$$u(z,\omega)=\pi N_a\frac{z}{f+z}=\omega\frac{a^2}{2cf}\frac{z}{f+z}. \quad (7)$$

It is worth writing Eq. (7) as $u(z,\omega)=\omega T_a(z)$, where

$$T_a(z)=\frac{a^2}{2cf}\frac{z}{f+z}. \quad (8)$$

Substituting Eq. (6) into Eq. (3) one can obtain the electric field on the optical axis in the vicinity of the focus by

$$E(z,t_A)=\frac{E_0f}{z}T_a(z)\mathcal{F}^{-1}_{t_A\omega}\times\left\{i\omega H(\omega)\frac{e^{-\kappa+i\omega T_a(z)}-1}{-\kappa+i\omega T_a(z)}e^{-i\omega(\Delta+f)/c}\right\}. \quad (9)$$

Shifting the origin of the time, i.e., introducing a new time variable t defined by

$$t=t_A-\frac{\Delta+f}{c}, \quad (10)$$

and using the properties of the Fourier transform, from Eq. (9) the electric field is given by

$$E(z,t)=\frac{E_0 f}{z}T_a(z)\mathcal{F}^{-1}_{\xi\omega}\left\{ i\omega H(\omega)\frac{e^{-\kappa+i\omega T_a(z)}-1}{-\kappa+i\omega T_a(z)}\right\}_{\xi=t-z/c} \tag{11a}$$

$$=\frac{E_0 f}{z}T_a(z)\mathcal{F}^{-1}_{\xi\omega}\{H(\omega)G(\omega)\}_{\xi=t-z/c} \tag{11b}$$

$$=\frac{E_0 f}{z}T_a(z)\{h(\xi)\otimes g(\xi)\}_{\xi=t-z/c}, \tag{11c}$$

where the symbol $\otimes$ denotes the operation of convolution, $g(t)=\mathcal{F}^{-1}_{t\omega}\{G(\omega)\}$ and

$$G(\omega)=i\omega\frac{e^{-\kappa+i\omega T_a(z)}-1}{-\kappa+i\omega T_a(z)}. \tag{12}$$

After long, but straightforward calculation one can show that

$$g(t)=\begin{cases}\dfrac{1-e^{-\kappa}}{\kappa}b'(t), & \text{if} \quad T_a=0,\\ \dfrac{\kappa}{T_a}e^{(\kappa/T_a)t}b(t)+\dfrac{e^{-\kappa}\delta(t+T_a)-\delta(t)}{T_a}, & \text{otherwise,}\end{cases} \tag{13}$$

where $\delta(t)$ is the Dirac delta function and $b(t)$ is defined by

$$b(t)=\begin{cases}\delta(t), & \text{if} \quad T_a=0,\\ 1/|T_a|, & \text{if} \quad T_a<0 \quad \text{and} \quad 0\leqslant t\leqslant -T_a,\\ 1/T_a, & \text{if} \quad T_a>0 \quad \text{and} \quad -T_a\leqslant t\leqslant 0,\\ 0, & \text{otherwise}\end{cases} \tag{14}$$

(see Fig. 3 in Ref. [28]). Please note that $b(t)$ [and consequently $g(t)$] differs from zero on the interval $[0,-T_a]$ in case of $T_a<0$, or $[-T_a,0]$ if $T_a>0$. Substituting Eq. (13) into Eq. (11) one can obtain

$$E(z,t)=\begin{cases}\dfrac{E_0 a^2}{2cf}\dfrac{1-e^{-\kappa}}{\kappa}h'(t), & \text{if} \quad z=0,\\ \dfrac{E_0 f}{z}\left[e^{-\kappa}h(\xi+T_a)-h(\xi)+\dfrac{\kappa}{T_a}\displaystyle\int_{\xi}^{\xi+T_a}h(\mu)e^{\kappa(\xi-\mu)/T_a}d\mu\right]_{\xi=t-z/c}, & \text{otherwise}\end{cases} \tag{15}$$

by calculating the convolution with $g(\xi)$.

A. Limiting cases

There are two important limiting cases depending on the value of truncation coefficient κ. In case of weak truncation of the input beam [i.e., $\kappa=(a/w)^2\gg 1$] Eq. (11) results in

$$E_g(z,t)=\frac{E_0 f}{z}T_w(z)\mathcal{F}^{-1}_{\xi\omega}\left\{\frac{i\omega H(\omega)}{i\omega T_w(z)-1}\right\}_{\xi=t-z/c} \tag{16a}$$

$$=\frac{E_0 f}{z}T_w(z)\mathcal{F}^{-1}_{t\omega}\left\{\frac{\omega H(\omega)}{1+[\omega T_w(z)]^2}e^{i[\arctan(\omega T_w(z))-(\omega/c)z+\pi/2]}\right\} \tag{16b}$$

$$=\begin{cases}\dfrac{E_0 w^2}{2cf}h'(t), & \text{if} \quad z=0,\\ \dfrac{E_0 f}{z}\left[\dfrac{1}{T_w}\displaystyle\int_{\xi}^{\pm\infty}h(\mu)e^{(\xi-\mu)/T_w}d\mu-h(\xi)\right]_{\xi=t-z/c}, & \text{otherwise,}\end{cases} \tag{16c}$$

where in the upper limit of the integral the minus sign should be used if $z<0$ and the plus sign if $z>0$. Here T_w is a newly introduced variable given by

$$T_w(z)=\frac{w^2}{2cf}\frac{z}{f+z}. \tag{17}$$

The other extreme case is the strong truncation of the incoming beam. If $\kappa \ll 1$ the electric field can be calculated from Eq. (11) [or Eq. (15)] assuming $\kappa \to 0$ (while a is fixed):

$$E_h(z,t) = \frac{2E_0 f}{z} \mathcal{F}^{-1}_{t\omega} \left\{ H(\omega) \sin \frac{\omega T_a(z)}{2} e^{i[\omega T_a(z)/2 - (\omega/c)z + \pi/2]} \right\} \tag{18a}$$

$$= \begin{cases} \dfrac{E_0 a^2}{2cf} h'(t), & \text{if} \quad z = 0, \\ \dfrac{E_0 f}{z} [h(t - z/c + T_a) - h(t - z/c)], & \text{otherwise.} \end{cases} \tag{18b}$$

This expression is identical with Eq. (18) in Ref. [28] where $N_a \gg 1$ and a homogeneous illumination of the lens was assumed. Equations (15) and (8) can be regarded as the generalization of Eqs. (18) and (10) in Ref. [28], respectively. The first term between bracket in Eq. (15) is the manifestation of the boundary waves generated by the aperture. It can be shown that $e^{-\kappa} h(t - z/c + T_a)$ describes a disturbance originated from the boundary of the aperture [29]. This disturbance was called boundary wave pulse in [28,30].

B. Causality

The causality of a linear system can be ascertained from the impulse response function (or Green function) of the system which is the response of the system to the $\delta(t)$ input. The impulse response function can be calculated from Eq. (11) assuming $h(t) = \delta(t)$. It is given by

$$\mathcal{G}(z,t) = \frac{E_0 f}{z} T_a(z) \{ \delta(\xi) \otimes g(\xi) \}_{\xi = t - z/c} = \frac{E_0 f}{z} T_a(z) g(t - z/c) \tag{19a}$$

$$= \begin{cases} \dfrac{E_0 a^2}{2cf} \dfrac{1 - e^{-\kappa}}{\kappa} \delta'(t), & \text{if} \quad z = 0, \\ \dfrac{E_0 f}{z} [e^{-\kappa} \delta(\xi + T_a) - \delta(\xi) + \kappa e^{(\kappa/T_a)\xi} b(\xi)]_{\xi = t - z/c}, & \text{otherwise,} \end{cases} \tag{19b}$$

where in the last step Eq. (13) was used. As it was mentioned before, function $b(t)$ is exactly zero outside the interval $[0, -T_a]$ in case of $T_a < 0$ ($z < 0$), or $[-T_a, 0]$ if $T_a > 0$ ($z > 0$). So, on the optical axis at a point P given by z, $\mathcal{G}(z,t)$ differs zero on a time interval

$$\mathcal{T}(z) = \begin{cases} [z/c, z/c - T_a(z)], & \text{if} \quad z < 0, \\ [z/c - T_a(z), z/c], & \text{otherwise,} \end{cases} \tag{20}$$

and exactly zero outside. It can be shown that $\mathcal{T}(z)$ is exactly the time interval in which the disturbance occurred on surface S passes through at point P, which means that the causality is not violated. According to our assumption the pulse front fills surface S (see Fig. 1) at $t = -f/c$. A sudden disturbance arisen at a typical point Q of surface S propagating with velocity c reaches point P at

$$t = -f/c + s/c. \tag{21}$$

At the calculation of the spectral components $U(z,\omega)$ [Eq. (6)] the distance s was approximated by

$$s = (f+z) \left[1 - \frac{1}{2} \left(\frac{\rho}{f+z} \right)^2 \frac{z}{f} - \cdots \right] = f + z - cT_\rho(z) \tag{22}$$

[see Eq. (2.9) and the paragraph below the equation in Ref. [27]] where $T_\rho(z)$ is a new variable with dimension of time given by

$$T_\rho(z) = \frac{\rho^2}{2cf} \frac{z}{f+z}. \tag{23}$$

From Eq. (22) one can see the physical meaning of $T_\rho(z)$: it gives the time difference between the axial and the QP path. Specially for the marginal path, that is when point Q lies at the edge of surface S the time difference is $T_a(z) = a^2/(2cf) \cdot z/(f+z)$. Substituting Eq. (22) into Eq. (21) one can obtain that the disturbance reaches point P at the moment

$$t = z/c - T_\rho(z) = z/c - (\rho/a)^2 T_a(z). \tag{24}$$

From the relation of $0 \leqslant \rho \leqslant a$ follows that the set of the moments defined by Eq. (24) coincide with the time interval $\mathcal{T}(z)$. Equation (24) has the following clear physical meaning. An observer at an axial point $P \neq F$ (i.e., $z \neq 0$) could see that in the time interval of $\mathcal{T}(z)$ light comes from a sharp bright ring on the screen of the aperture. Equation (24) gives the radius of the ring:

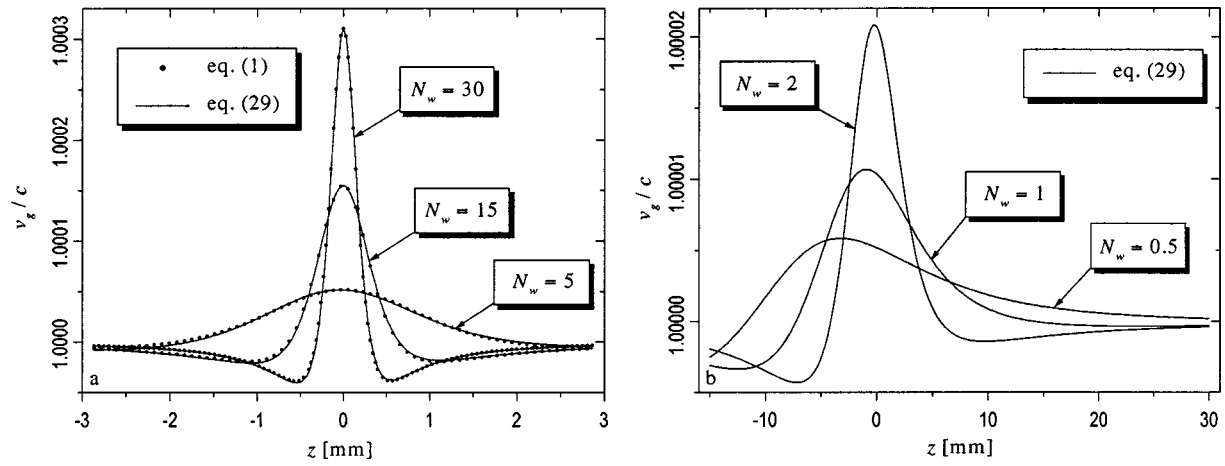

FIG. 2. The group velocity on the optical axis in case of weak truncation of the incoming beam for various values of the Fresnel number associated with beam waist at the lens. For small values of N_w the curves are asymmetric and the maximum is shifted towards the aperture.

$$\rho(z,t)=a\sqrt{\frac{z/c-t}{T_a(z)}}, \tag{25}$$

where $t\in\mathcal{T}(z)$. From Eq. (25) one can see that if $z<0$ the radius of the ring increases in time from 0 to a, and if $z>0$ the radius of the ring decreases in time from a to 0. Which means that in front of the focus ($z<0$) the disturbance arrives first along the axial and finally along the marginal path, and behind the focus ($z>0$) it arrives in reverse order. The superluminality treated below is caused by the interference of the secondary wavelets risen from the wave front which fills the aperture at the moment $t=-f/c$ (Huygens-Fresnel principle). The light waves propagating in different paths cause a reshaping process of the wave packet likewise the probability waves described in Ref. [22].

III. GROUP VELOCITY

First we will calculate the group velocity for the two limiting cases and then (in the following section) the physical meaning of the group velocity and the pulse shape during the propagation will be discussed. The group velocity [31] on the optical axis is defined by

$$v_g(z)=-\left[\frac{\partial}{\partial z}\frac{\partial\Phi}{\partial\omega}\bigg|_{\omega_0}\right]^{-1}, \tag{26}$$

where $\Phi=\Phi(z,\omega)$ is the phase of the field. Equation (26) follows from the expression of

$$t+\frac{\partial\Phi}{\partial\omega}\bigg|_{\omega_0}=0, \tag{27}$$

which gives implicitly the position of a hypothetical point M moving with speed $v_g(z)$ along the optical axis. Point M is usually the point at which the absolute amplitude of the field attains its maxima at time t. The phase of the field for the two limiting cases will be denoted by Φ_g and Φ_h for cases weak and strong truncation of the incident pulsed beam, respectively.

A. Weak truncation

In case of weak truncation from Eq. (16) the phase is given by

$$\Phi_g(z,\omega)=\arctan(\omega T_w(z))-(\omega/c)z+\pi/2. \tag{28}$$

Substituting Eq. (28) into Eq. (26) the group velocity has the form

$$v_g(z)=\frac{[1+[\omega_0T_w(z)]^2]^2c}{[1+[\omega_0T_w(z)]^2]^2-[1-[\omega_0T_w(z)]^2]cT_w'(z)} \tag{29a}$$

$$=\frac{[1+[\pi N_w z/(f+z)]^2]^2c}{[1+[\pi N_w z/(f+z)]^2]^2-[1-[\pi N_w z/(f+z)]^2]\dfrac{w^2}{2(f+z)^2}}, \tag{29b}$$

which is the generalization of Eq. (1) for any values of N_w. Figure 2 shows the group velocity at central wavelength $\lambda_0 = 620$ nm on the optical axis of a lens with focal length $f = 30$ mm for various values of N_w. The results of Eq. (29) and Eq. (1) were plotted with solid lines and circles, respectively. One can see that Eq. (1) is a good approximation of Eq. (29) for large values of N_w. For small values of N_w the curves become asymmetric and the maximum is shifted towards the lens likewise the focal shift. The group velocity is still greater than c in the vicinity of the maximum. From Eq. (28) and Eq. (27) one can obtain that point M moving on the axis reaches point P (given by z) at time

$$t_g(z) = \frac{z}{c} - \frac{T_w(z)}{1+[\omega_0 T_w(z)]^2}. \tag{30}$$

B. Strong truncation

Unlike the weak truncation of the incoming beam (when a well behaved function gives the phase distribution) in case of strong truncation the phase has discontinuity of π at each axial point of the zero intensity [see Eq. (18)]. From Eq. (18) the phase of the focused beam is given by

$$\Phi_h(z,\omega) = \omega T_a(z)/2 - (\omega/c)z + \pi/2 + K, \tag{31}$$

where $K=0$ if $\sin(\omega T_a(z)/2)>0$, and $K=\pi$ if $\sin(\omega T_a(z)/2)<0$. Because of the discontinuities we have to exclude the axial points given by $\sin(\omega_0 T_a(z)/2)=0$ in use of Eq. (26). Except these points one obtains the group velocity as

$$v_g(z) = \frac{c}{1-\dfrac{a^2}{4(f+z)^2}}. \tag{32}$$

Because of the irregular behavior of the phase the physical meaning of Eq. (32) is doubtful. We will see that Eq. (32) gives the velocity of the centroid of the intensity.

IV. RESHAPING OF THE PULSE

In the foregoing the group velocity for the two limiting cases has been calculated. It has been shown that the group velocity exceeds c in the vicinity of the focal point. Therefore it is interesting to verify whether the peak of the intensity propagates with the group velocity. It is also an interesting question if pulse distortions occur during the propagation. Using Eq. (15) one can calculate the pulse shape during the propagation.

A. Weak truncation

In order to calculate the integral in Eq. (15) [or Eq. (16)] analytically, two special input pulse shapes were chosen. We would like to emphasize that the only reason of that choice of the envelopes is to avoid the numerical integration of Eq. (15). Other temporal pulse shapes (for example Gaussian) have been treated numerically. The numerical calculation

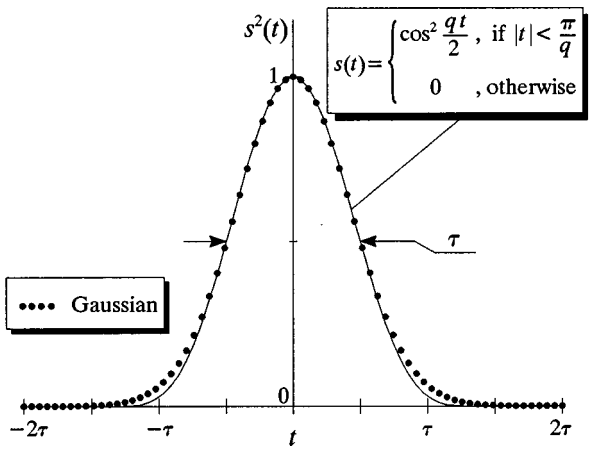

FIG. 3. Comparison between the input temporal pulse shape used in the analytical calculations and a Gaussian pulse with the same duration τ.

shows that the pulses with different temporal shapes exhibit exactly the same behavior described below. In case A the envelope was supposed to be

$$s(t) = \begin{cases} \cos^2\dfrac{qt}{2}, & \text{if} \quad |t|<\pi/q, \\ 0, & \text{otherwise}, \end{cases} \tag{33}$$

where q is a scale factor given by $q = 2\arccos(\sqrt{2}-1)/\tau$. This type of pulse shape [Eq. (33)] was compared with a Gaussian pulse with the same duration τ in Fig. 3. The function described by Eq. (33) is continuous and differentiable. In case B an exponentially rising and falling envelope was considered:

$$s(t) = e^{-\ln 2|t|/\tau}. \tag{34}$$

In this case the envelope is continuous but not differentiable at $t=0$. For the two envelopes the intensity was calculated using Eq. (15) with the following parameters: $\lambda_0 = 620$ nm, $\tau = 10$ fs, $f = 30$ mm, $a = 9$ mm, $w = 3$ mm. The temporal profile of the input pulse was depicted for the two cases (A and B) in the top corners of Fig. 4. Between them the time delay defined by

$$\Delta t(z) = t_g(z) - \frac{z}{c} = -\frac{T_w(z)}{1+[\omega_0 T_w(z)]^2} \tag{35}$$

was plotted. $\Delta t(z)$ can be regarded as a physical quantity which measures the amount of the anomaly of the arrival at a point z. Below the time dependence of the intensity at five points [denoted by (a)–(e)] of the optical axis was depicted with solid line. The circles show the intensity belonging to the input pulse (it was shifted and scaled to the maximum). The insets show the 1 fs wide interval of the maximum. In case A the peak of the intensity propagates with speed of v_g and there is no temporal distortion. For Gaussian pulse shape the same behavior was obtained by evaluating Eq. (15) numerically. While in case B the maximum (which is a break point) propagates with speed of c and pulse distortion occurs. In case of weak truncation it can be shown [using Eq. (16)

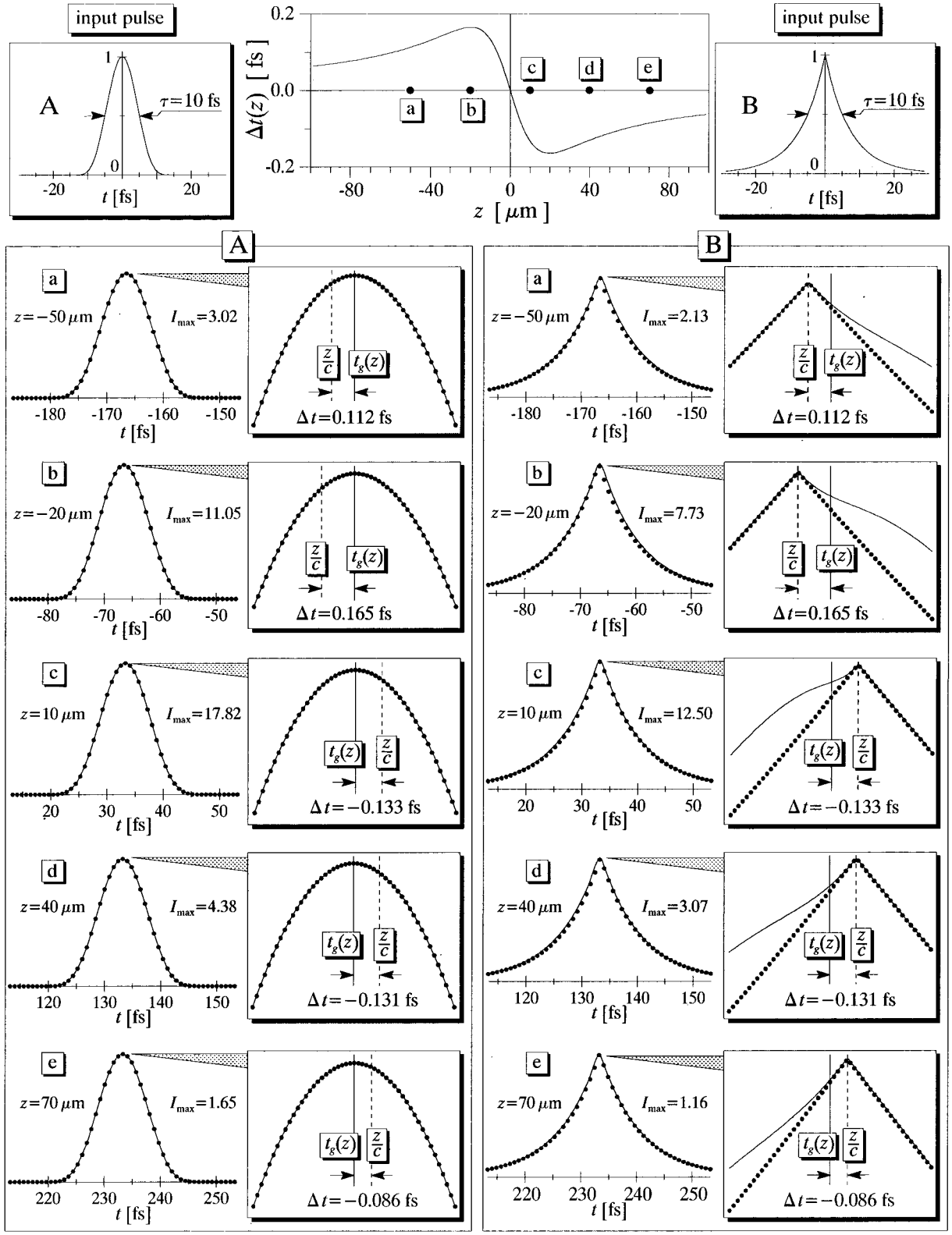

FIG. 4. Time dependence of the intensity (solid line) at five points [denoted by (a)–(e)] of the optical axis for two temporal pulse shapes (*A* and *B* shown in the top corners) assuming weak truncation of the incoming beam. The circles show the input temporal shape (shifted and scaled to the maximum). The insets show the 1 fs wide interval of the maximum. The delay $\Delta t(z)=t_g(z)-z/c$ is a physical quantity which measures the amount of the anomaly of the arrival at a point *z*.

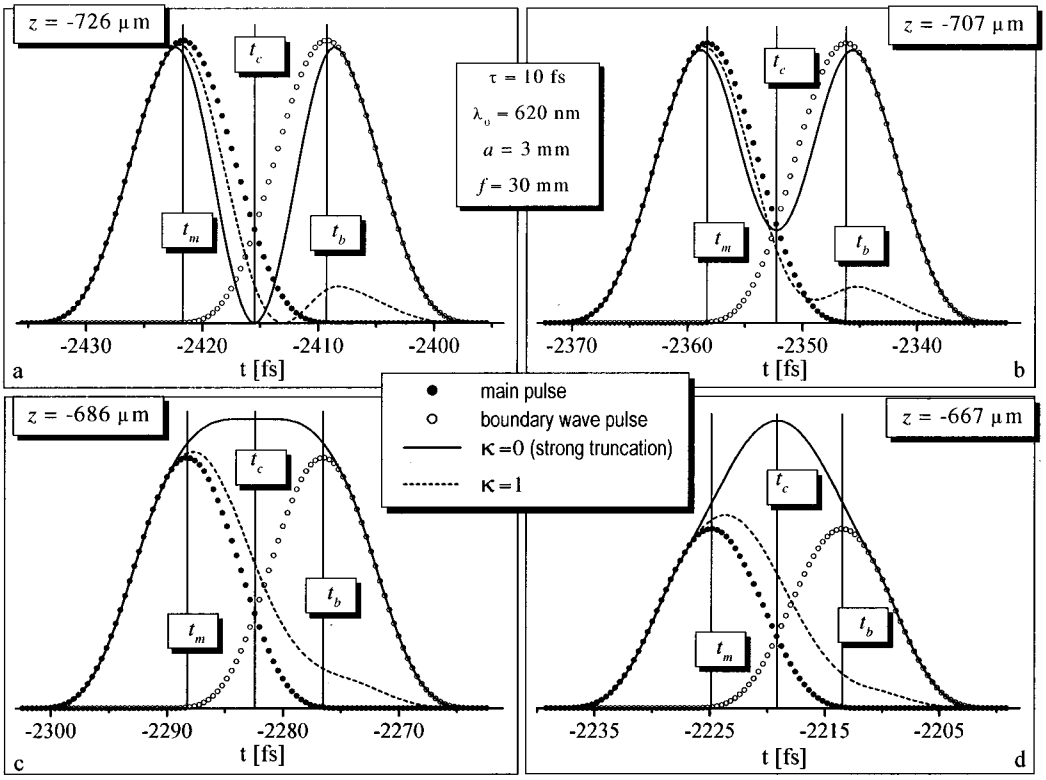

FIG. 5. In case of strong truncation of the incoming beam the main (black circles) and the boundary wave (hollow circles) pulse interfere. The intensity resulting from the interference is plotted with solid line [(a) destructive; (d) constructive interference; (b),(c) intermediate cases]. The dashed line indicates the intensity relating to the unity truncation coefficient.

and the properties of the integral function] that the break points and the discontinuities of the field move with speed of c.

B. Strong truncation

In case of strong truncation two pulses propagate on the optical axis [see Eq. (18)]. One of the pulses propagates with speed of c. It was called main pulse in Refs. [28,30]. The main pulse reaches point z at time $t_m = z/c$. The other pulse named boundary wave pulse arrives at the moment $t_b = z/c - T_a(z)$. The time difference between the two pulses is $T_a(z)$ [Eq. (8)]. The intensity on the optical axis is given by $I(z,t) = |E(z,t)|^2$. Using Eq. (18) and $h(t) = s(t)e^{i\omega_0 t}$ one can obtain

$$I(z,t) = (E_0 f/z)^2 [s^2(t-t_m) + s^2(t-t_b) - 2s(t-t_m)s(t-t_b)\cos(\omega_0 T_a)]. \tag{36}$$

This expression shows that the main and the boundary wave pulse interfere. The interference term is the last term between the (square) brackets in Eq. (36). Destructive interference occurs at points z given by $\omega_0 T_a(z) = 2m\pi$, where $m = \pm 1, \pm 2, \ldots$. The interference is constructive at points where the condition $\omega_0 T_a(z) = (2m+1)\pi$ is satisfied with $m = 0, \pm 1, \pm 2, \ldots$. The intensity varies between $(E_0 f/z)^2 [s(t-t_m) - s(t-t_b)]^2$ and $(E_0 f/z)^2 [s(t-t_m) + s(t-t_b)]^2$. Figures 5(a) and 5(d) show destructive and constructive interference, respectively. (The parameters of the calculations are $\lambda_0 = 620$ nm, $\tau = 10$ fs, $f = 30$ mm, $a = 3$ mm.) Two intermediate cases are plotted in Figs. 5(b) and 5(c). The intensity of the main and the boundary wave pulse is depicted by small circles. The dashed line indicates the intensity belonging to unity truncation parameter κ $(w = a)$. In this case the amplitude of the boundary wave pulse is smaller, which reduces its influence. If $s(t)$ is an even function, the pulse centroid defined by

$$t_c(z) = \int_{-\infty}^{\infty} t|E(z,t)|^2 dt \Big/ \int_{-\infty}^{\infty} |E(z,t)|^2 dt \tag{37}$$

may be expressed in the form

$$t_c(z) = \frac{t_m + t_b}{2} = \frac{z}{c} - \frac{T_a(z)}{2}. \tag{38}$$

From Eq. (38) the velocity of the pulse centroid is given by

$$v_c(z) = \left[\frac{dt_c}{dz}\right]^{-1} = \frac{c}{1 - \dfrac{a^2}{4(f+z)^2}}, \tag{39}$$

which is identical with Eq. (32). That is, if $s(t)$ is even, the pulse centroid moves on the optical axis with speed of v_g.

Approaching the focus the time difference between the main and the boundary wave pulse decreases. The two pulses construct only one pulse propagating with speed of v_c. In Fig. 6(a) the solid line shows the time dependent intensity at $z = -15$ μm. The circles indicate the input intensity profile

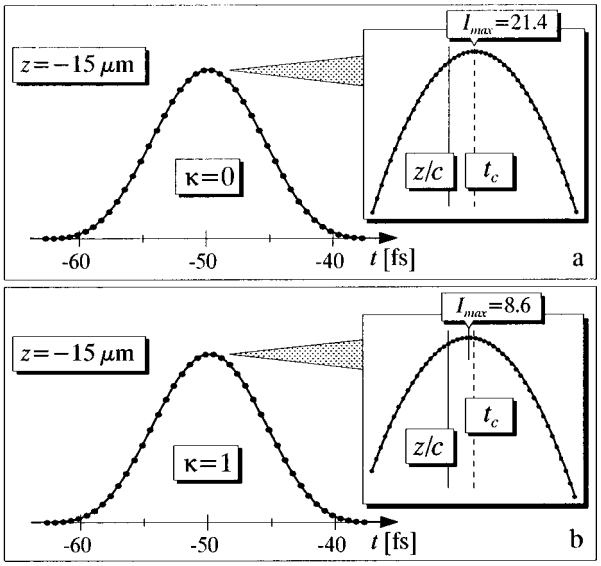

FIG. 6. Approaching the focus, the interference between the main and the boundary wave pulse yields only one pulse (solid line). The circles indicate the input intensity profile scaled and shifted to the maximum. The inset shows 1 fs wide time interval of the maximum. The intensity reaches its maximum at t_c (a) in case of $\kappa=0$ (strong truncation), while between z/c and t_c in case of $\kappa=1$ (b).

scaled and shifted to the maximum. The inset shows 1 fs wide time interval of the maximum. Using the expansion of $\cos(x)=1-x^2/2+\cdots$ one can obtain an approximation of Eq. (36) for small values of z:

$$I(z,t)\approx\left[\frac{E_0a^2}{2c(f+z)}\right]^2[[s'(t-t_c)]^2+[\omega_0 s(t-t_c)]^2]$$
$$\approx\left[\frac{E_0a^2\omega_0}{2c(f+z)}s(t-t_c)\right]^2, \qquad (40)$$

where the last approximation is valid for $(\omega_0\tau)^2\gg 1$. Equation (40) describes a pulse propagating with speed of v_c.

In Fig. 6(b) the solid line shows the intensity at $z=-15$ μm depending on the time for unity truncation parameter κ. The circles indicate the input intensity profile scaled and shifted to the maximum. The inset shows 1 fs wide time interval of the maximum. The intensity reaches its maximum between z/c and t_c which means that the speed of the maximum differs from c.

V. CONCLUSIONS

It has been pointed out that the phase anomaly leads to superluminal propagation of femtosecond pulses. The group velocity for the two important limiting cases has been calculated and its physical meaning discussed. Analytical expressions have been derived for the electric field on the optical axis. The causality of the system has been proved. The superluminality is the result of the pulse reshaping caused by the Gouy phase shift.

Although we have considered an aberration-free lens here, the effect occurs in case of other (aberration-free) focusing systems. The Gouy shift is caused by the truncation of the converging spherical wave fronts by the aperture. We have used scalar approximation, but it is known if $\lambda\ll a$ and $a^2\ll f^2$, the scalar treatment is adequate and is in agreement with the experimental results.

ACKNOWLEDGMENTS

This work has been supported by OTKA Grant Nos. F020889 and T016631, World Bank–OTKA Grant No. W015239, and FKFP Grant No. 0208/97.

[1] M. Born and E. Wolf, *Principles of Optics*, 6th (corrected) ed. (Pergamon Press, Oxford, 1987), Chap. 8.8.
[2] A. E. Siegman, *Lasers* (University Science Books, Mill Valley, CA, 1986), p. 645.
[3] J. Jones, Am. J. Phys. **42**, 43 (1974).
[4] Z. L. Horváth, J. Vinkó, Zs. Bor, and D. Von der Linde, Appl. Phys. B: Lasers Opt. **63**, 481 (1996).
[5] L. Brillouin, *Wave Propagation and Group Velocity* (Academic Press, New York, 1960).
[6] K. E. Oughstun and G. C. Sherman, *Electromagnetic Pulse Propagation in Causal Dielectrics* (Spinger-Verlag, Berlin, 1994).
[7] R. Y. Chiao and A. M. Steinberg, in *Tunneling Times and Superluminality*, Progress in Optics Vol. XXXVII, edited by E. Wolf (Elsevier, Amsterdam, 1997), p. 345.
[8] G. Nimtz and W. Heitmann, Prog. Quantum Electron. **21**, 81 (1997).
[9] C. G. B. Garrett and D. E. McCumber, Phys. Rev. A **1**, 305 (1970).
[10] R. Y. Chiao, Phys. Rev. A **48**, R34 (1993).
[11] R. Y. Chiao and J. Boyce, Phys. Rev. Lett. **73**, 3383 (1994).
[12] R. Y. Chiao, J. Boyce, and M. W. Mitchell, Appl. Phys. B: Lasers Opt. **B60**, 259 (1995).
[13] E. L. Bolda, J. C. Garrison, and R. Y. Chiao, Phys. Rev. A **49**, 2938 (1994).
[14] E. L. Bolda, Phys. Rev. A **54**, 3514 (1996).
[15] R. Y. Chiao, A. E. Kozhekin, and G. Kurizki, Phys. Rev. Lett. **77**, 1254 (1996).
[16] A. Enders and G. Nimtz, Phys. Rev. B **47**, 9605 (1993).
[17] A. Ranfagni, P. Fabeni, G. P. Pazzi, and D. Mugnai, Phys. Rev. E **48**, 1453 (1993).
[18] A. Ranfagni and D. Mugnai, Phys. Rev. E **54**, 5692 (1996).
[19] D. Mugnai, A. Ranfagni, and L. S. Schulman, Phys. Rev. E **55**, 3593 (1997).
[20] A. M. Steinberg, P. G. Kwiat, and R. Y. Chiao, Phys. Rev. Lett. **71**, 708 (1993).
[21] Ch. Spielmann, R. Szipőcs, A. Stingl, and F. Krausz, Phys. Rev. Lett. **73**, 2308 (1994).
[22] W. Yun-ping and Z. Dian-lin, Phys. Rev. A **52**, 2597 (1995).
[23] Y. Japha and G. Kurizki, Phys. Rev. A **53**, 586 (1996).

[24] R. Pelster, V. Gasparian, and G. Nimtz, Phys. Rev. E **55**, 7645 (1997).
[25] M. Blaauboer, A. G. Kofman, A. E. Kozhekin, G. Kurizki, D. Lenstra, and A. Lodder, Phys. Rev. A **57**, 4905 (1998).
[26] Y. Li and E. Wolf, Opt. Commun. **39**, 211 (1981).
[27] Y. Li and E. Wolf, Opt. Commun. **42**, 151 (1982).
[28] Z. L. Horváth and Zs. Bor, Opt. Commun. **108**, 333 (1994).
[29] Z. L. Horváth and Zs. Bor (unpublished).
[30] Zs. Bor and Z. L. Horváth, Opt. Commun. **94**, 249 (1992).
[31] M. Born and E. Wolf, *Principles of Optics* (Ref. [1]), Chap. 1.3.4.